LETTER Communicated by Peter König

Integrator or Coincidence Detector: A Novel Measure Based on the Discrete Reverse Correlation to Determine a Neuron's Operational Mode

Jacob Kanev
jkanev@zoho.com
Institute of Software Engineering and Theoretical Computer Science, Technische Universität Berlin, Berlin 10587, Germany

Achilleas Koutsou
achilleas.k@cs.ucy.ac.cy
Chris Christodoulou
cchrist@cs.ucy.a.cy
Department of Computer Science, University of Cyprus, 1678 Nicosia, Cyprus

Klaus Obermayer
klaus.obermayer@mailbox.tu-berlin.de
Institute of Software Engineering and Theoretical Computer Science, Technische Universität Berlin, Berlin 10587, Germany

In this letter, we propose a definition of the operational mode of a neuron, that is, whether a neuron integrates over its input or detects coincidences. We complete the range of possible operational modes by a new mode we call gap detection, which means that a neuron responds to gaps in its stimulus. We propose a measure consisting of two scalar values, both ranging from -1 to $+1$: the neural drive, which indicates whether its stimulus excites the neuron, serves as background noise, or inhibits it; the neural mode, which indicates whether the neuron's response is the result of integration over its input, of coincidence detection, or of gap detection; with all three modes possible for all neural drive values. This is a pure spike-based measure and can be applied to measure the influence of either all or subset of a neuron's stimulus. We derive the measure by decomposing the reverse correlation, test it in several artificial and biological settings, and compare it to other measures, finding little or no correlation between them. We relate the results of the measure to neural parameters and investigate the effect of time delay during spike generation. Our results suggest that a neuron can use several different modes simultaneously on different subsets of its stimulus to enable it to respond to its stimulus in a complex manner.

Neural Computation **28, 2091–2128** (2016)
doi:10.1162/NECO_a_00875

1 Introduction

For a considerable time, there has been a discussion about whether a neuron acts as a coincidence detector or an integrator. Despite a number of contributions on this issue, the underlying assumption about what is actually meant by the terms *integrator* or *coincidence detector* seems to have varied.

The discussion was sparked off by Abeles (1982), who stated that the cortical neuron is a coincidence detector, not an integrator. This was based on the fact that the neuron is usually more sensitive to a few spikes that arrive at the same time than to the same number of spikes when they are distributed over a longer time. He used a measure he called *coincidence advantage* that shows the extent to which synchronous activation of a few synapses is more effective than asynchronous activation of the same synapses. Kempter, Gerstner, and van Hemmen (1998) used a similar measure that expresses the ratio of the neuron's response rates to either random or correlated stimulus.

The coincidence advantage measure, introduced by Abeles (1982), uses a neuron model with a threshold and an exponential rise after the reset, and it assumes gaussian-distributed excitatory stimulus. A distinction is made between the background stimulus, which is used to keep the membrane potential at its average rate, and the signal stimulus, which is or is not detected by the postsynaptic neuron. He defines three values: the *synchronous attenuation* is the number of simultaneous stimulus spikes necessary to get the membrane potential from its average voltage to threshold voltage. The *asynchronous attenuation* is the number of nonsimultaneous stimulus spikes, additional to the background, that are needed to get one additional response spike. Finally, the coincidence advantage is defined as the ratio of synchronous attenuation to asynchronous attenuation.

Some subsequent contributions were based on the mean and variance of the response spike train. Softky and Koch (1993) argued that in integration mode, the resulting spike train should be regular at high firing rates, while the high firing irregularity that is observed in cortical neurons means the neuron is detecting coincidences. These authors used the *coefficient of variation* (CV) to characterize the high firing irregularity and defined it as the standard deviation of the stimulus interspike interval, divided by the mean stimulus interspike interval. In their paper, the coincidence detection mode is equivalent to the neuron reacting to occasional input bursts with a single response, where in between responses, the neuron forgets previous inputs because the membrane potential polarizes again. Similarly, Bell, Mainen, Tsodyks, and Sejnowski (1995) tried to explain the high CV observed in cortical neurons at high rates and found a balanced parameter regime in which high CVs can be observed. They concluded that a high-response CV is not observed when a neuron mainly integrates on its input. In their work, the high CV was seen as an indirect measure that a neuron is not integrating. Stevens and Zador (1998) also used the CV as an indirect

indicator for a coincidence detection scenario and claimed that the high CV that is observed in neurons in vivo at high rates is the result of synchronous stimulus, indicating a coincidence detection scenario.

Other authors based their reasoning on the integration time of the neuron. König, Engel, and Singer (1996) suggested that the distinction between the two modes could be made by the ratio of the integration time interval of the neuron and its response interspike interval (ISI). In integration mode, a neuron has a long integration interval compared to its response rate, while in coincidence detection, it is short. The membrane time constant can be lowered significantly by background stimulus activity, making coincidence detection plausible even in regimes where the response firing rate is higher than 25 Hz. The *integration time window* measure, introduced by König et al. (1996), is defined as the ratio of a neuron's integration time window to the response interspike interval. The integration time window is equal to the membrane time constant τ in the exponential rise $\exp(-\frac{t}{\tau})$ of the membrane potential. König et al. (1996) also showed that correlated excitatory and inhibitory stimulus has the same effect of inducing coincidence detection mode. Shadlen & Newsome (1994, 1998) argue, in favor of a time window measure, that a high CV does not show neurons to be coincidence detectors, because a high CV can be reached by balanced excitation and inhibition. Due to the high number of connections to a neuron, a population code is predominant in the mammalian cortex. Instead of the CV, a time window measure should be used where integrators are characterized by a long time constant and coincidence detectors by a short one. Ratté, Lankarany, Rho, Patterson, and Prescott (2015) analyzed subthreshold mechanisms that lead to coincidence detection or integration mode. In addition to these two modes, they introduce a differentiation mode, where a response is triggered whenever there is a sudden rate increase in an otherwise steady stimulus. Integration mode in their work is characterized by a long integration time window and regular response, while coincidence detection is characterized by a short time window and immediate response after a coincidence in the stimulus.

Other authors suggested using time windows on the stimulus. Bugmann, Christodoulou, and Taylor (1997) demonstrated that a partial reset model can explain the high CV in high mean responses, that temporal integration and coincidence detection can coexist, and that reverse correlation curves fail to show whether a neuron is in integration or coincidence detection mode. Here coincidence detection is equivalent to the presence of simultaneous spikes that cause the neuron to fire in a small time window before the response. Roy and Alloway (2001) found by in vivo studies that neurons in the cortex are possibly reacting to synchronous thalamic discharges. To distinguish coincidence detection from temporal integration, they used a time window approach to classify stimuli as synchronous or asynchronous and then calculated the correlation between either synchronous or asynchronous events and the response. Koutsou, Christodoulou, Bugmann, and

Kanev (2012) found that neurons can act as integrators even in a high-rate and high-response variance setting. They proposed a new measure, the *normalized prespike slope* (NPSS), based on the mean of a normalized membrane slope during a small time window before the response. More specifically, the NPSS is based on the mean slope of the membrane potential in the last n milliseconds before the response, n being a parameter of the method. That slope is normalized for each response spike, using a theoretical slope for perfect integration as a lower bound and a theoretical slope for perfect coincidence detection as an upper bound. The lower bound is defined as the slope that results if the response spike were the result of integration over constant input during the interresponse spike interval. The upper bound is defined as the slope that results if the neuron had received all its stimulus in the time window before the response. The linearly normalized slope is averaged over many responses, yielding the NPSS. A neuron is a perfect integrator if its membrane potential is driven to the threshold by a constant stimulus and a perfect coincidence detector if the membrane rises from the static mean to the threshold within the preresponse time window of n ms. In addition, Koutsou, Kanev, and Christodoulou (2013) investigated whether correlations in the input can be estimated by looking at the membrane potential and the neural response. They found that large parts of stimulus synchrony are reflected by a neuron's response. In that work, a neuron was considered to be a coincidence detector if the synchrony of the stimulus could be recreated from the neuron's response.

Investigations were also done using actual spike-wise input-output relations. Rudolph and Destexhe (2003) concluded that a neuron operates in continuum between both modes, and the main influence on the mode is synchrony in the stimulus. Using a compartmental model and stimulating with gaussian spike volleys of a certain standard deviation, they proposed a reliability measure R as the ratio of number of responses over number of spike volleys. In integration mode, a neuron responds with $R = 1$ to a stimulus with large standard deviation. In coincidence detection mode, a neuron responds with $R = 1$ to a stimulus with a small standard deviation. Kreuz, Haas, Morelli, Abarbanel, and Politi (2007), Kreuz, Chicharro, Andrzejak, Haas, and Abarbanel (2009), Kreuz, Chicharro, Greschner, and Andrzejak (2011), and Kreuz, Chicharro, Houghton, Andrzejak, and Mormann (2013) have suggested several stimulus correlation measures. While they make no claim about the predominant mode of cortical neurons, they underline the idea that synchrony plays an important role in neural coding. Kreuz, Mulansky, and Bozanic (2015) have suggested a new coincidence measure, the SPIKE-synchronization distance, and Mulansky, Bozanic, Sburlea, and Kreuz (2015) have investigated its mathematical properties. This measure is a pure similarity measure between neural spike trains and is not related to neural response modes. Here, a coincidence is a close pair of spikes from different neurons, distanced fewer than half of the previous or following interspike intervals in each of both neurons, respectively.

Considerably fewer studies looked at Fourier transformations of spike trains into frequency space. Hsu, Borst, and Theunissen (2004) argued that a rate-based code is at work in the cortex but with constantly changing rates. As a measure for the integration mode, they proposed a special form of coherence between stimulus and response. Ostojic, Brunel, and Hakim (2009) investigated the influence of various parameters on spike train correlations using a Fourier transform approach.

We believe that if a measure for the neural operational mode is to serve as a basis of a broad discussion and aid investigation and understanding of neural behavior, it should have certain properties: (1) it should be as general as possible—in particular, it should be independent of a specific neuron model, its parameters, or details of a real biological neuron to be measured; (2) it should be as simple as possible; and (3) the concept of a coincidence should be well defined and in a general and intuitive way.

In this letter, we try to clarify the concept of a neural operational mode. We propose a definition of the neural mode that is as simple and direct as possible, leading to a mathematical way to distinguish coincidence detection from temporal integration and to quantify what kind of influence a presynaptic spike train has had on a neuron's response.

In section 2, we derive a new definition from the standard reverse correlation and formulate the measure. In section 3, we present and discuss the measure's behavior under different conditions, in relation to existing measures and its performance on biological data. The letter finishes with a discussion of the measure, our results, and further implications in section 4. An appendix gives technical details of the numerical experiments.

2 Materials and Methods

2.1 Decomposing the Response-Stimulus Correlation. We base our measure of the neural operational mode on a decomposed form of the response-stimulus (or reverse) correlation (RSC). The RSC is estimated by averaging time windows of the stimulus that have the same length and are centered at observed response spikes. Continuous RSC shows the conditional mean stimulus just before a neuron's response. Unfortunately the RSC cannot show whether the neuron operates as a temporal integrator or a coincidence detector (Mainen & Sejnowski, 1995; Bugmann et al., 1997). To overcome this, we decompose the RSC into the contributions of the single spikes before a response.

Consider an ordered set of stimulus spike times

$$S = \{s_0 < s_1 < s_2 < \ldots\}$$

and an ordered set of response spike times

$$T = \{t_0 < t_1 < t_2 < \ldots\}$$

generated by a neuron. Let s_i be the time of the last stimulus spike before a response spike at t_j,

$$s_i = \max_k \{s_k | s_k < t_j\}.$$

Consider distances from the nth stimulus spike before t_j to t_j itself:

$$t_j - s_{i-n}.$$

These distances have a distribution (see Figure 1, middle). We calculate the temporal mean for each distribution separately,

$$R_n = \frac{1}{J} \sum_j (t_j - s_{i-n}),$$

where J is the number of response spikes used in the average; t_j are their times; and s_{i-n} are the times of the preceding nth stimulus spike before the response. The result is a decomposed discrete RSC, $R_n(T, S)$, a series of time distances to an observed response spike, where R_0 is the distance between the response and the last stimulus before the response, R_{-1} is the distance between the response and the penultimate stimulus before the response, and so on (see Figure 1, bottom).

Note, however, that if, instead of building temporal means per distribution, the distributions of the spike distances $t_j - s_{i-n}$ (see Figure 1, middle) are added up for each point in time separately and divided by the mean stimulus rate λ, they yield the normalized expected number of spikes at that certain time before the observed response spike. The result is the standard nondecomposed reverse correlation (see Figure 1, top).

As a last step we use the decomposed correlation R_n to define the time series r_n of stimulus intervals, where each r_n is the (positive-valued) time interval of the nth stimulus spike pair preceding a response,

$$\begin{aligned} r_0 &= -R_0, \\ r_1 &= R_0 - R_{-1}, \\ r_2 &= R_{-1} - R_{-2}, \\ &\cdots \\ r_n &= R_{-(n-1)} - R_{-n}. \end{aligned}$$

The first two elements of this series, r_0 and r_1, will form our proposed measure of the neuron's operational mode.

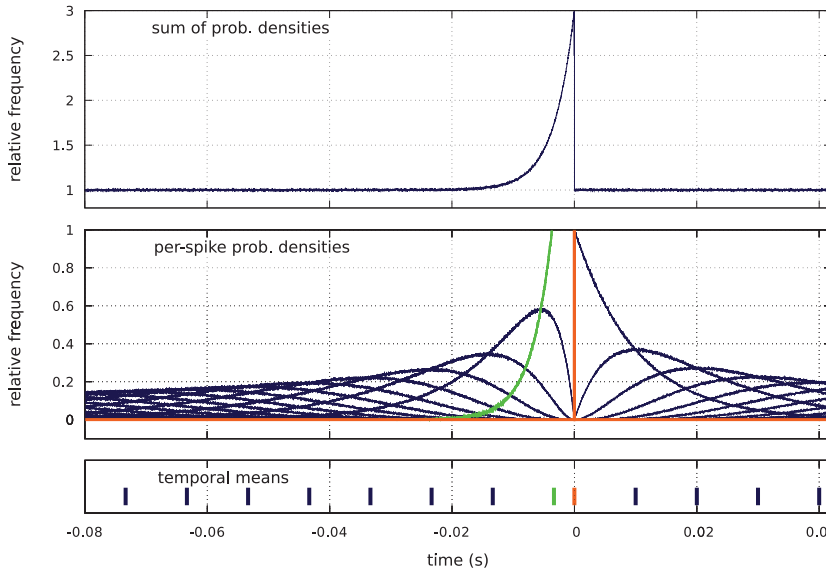

Figure 1: Decomposed response-stimulus correlation. (Top) Reverse correlation, built from single per-spike distributions of a simulated conductance-based neuron, as shown in the middle part. (Middle) Distributions of arrival times of the nth spike of the same neuron before the response. Adding all curves will result in the reverse correlation shown in the top part of the figure. (Bottom) Temporal mean of each of the single distributions from the middle panel. This is a decomposed discrete form of the RSC, showing the mean arrival time of each nth preresponse stimulus, as is used in our later analysis. The data was produced by a numerical simulation of a conductance-based integrate-and-fire neuron according to equation 3.1 with a reset of -50 mV (partial reset according to Bugmann et al., 1997), resting potential of -60 mV, membrane time constant of 20.0 ms, threshold of -42.0 mV, an excitatory conductance at 0 mV with synaptic weight of 0.3 driven by a Poisson process of rate 100 Hz, and an inhibitory conductance at -75 mV with synaptic weight of 0.6 driven by a Poisson process of rate 200 Hz.

2.2 Neural Mode and Drive. What is a neuron doing when it is considered to be integrating or detecting coincidences? We think the most natural answer would be to say that a neuron detects coincidences when it responds whenever spikes in its stimulus appear at the same time or are very close to each other. It integrates when it fires with a steady rate in response to fairly steady regular stimulus and its response rate somehow reflects the rate of its stimulus. The context of the whole spike train decides whether a succession of stimulus spikes is an episode of rapidity within an otherwise calm input or whether it is part of a totally homogeneous but high-rate

stimulus. Because of this, a neuron's operational mode measure must be independent of temporal scaling of both stimulus and response.

We define a neuron's neural drive as follows: (1) a neuron is positively driven by a stimulus when a response spike is fired almost immediately after the last preceding stimulus spike, (2) a neuron is negatively driven by a stimulus when the response delay after the last preceding stimulus spike is a lot longer than what is to be expected if the stimulus and response were independent processes, and (3) a neuron is not driven by a stimulus when the response delay after the last stimulus spike is what would be expected if both processes were independent. These correspond loosely to excitation (for positive drive), hyperpolarizing inhibition (for negative drive), and either independence or shunting inhibition (for no drive); differences will be made clear in section 3.

Looking at the last two stimulus spikes before a response, we define a neuron's operational mode as follows:

- Coincidence detection is the operational mode where the neural drive is positive and the neuron responds to pairs of stimulus spikes that are significantly closer than expected
- Integration is the operational mode where the neural drive is positive and the neuron responds to pairs of stimulus spikes that are an average time apart
- Gap detection is the operational mode where the neural drive is positive and the neuron responds to a pair of stimulus spikes that are significantly farther apart than expected.

The width of this last interval is relative to the rate of the stimulus in question.

Our proposed measure $R_{M,D}$ for the operational stimulus-response mode consists of these two values: the neural mode R_M, denoting gap detection/integration/coincidence detection, and the neural drive R_D denoting negative/positive drive. Both values should range from -1 to 1.

To achieve a range from -1 to 1 for the neural drive, the distance r_0 of the last stimulus spike to the response is normalized by dividing it by the expected distance if stimulus and response were independent and scaled exponentially so that when $r_0 = 0$, the mode is 1 (the neuron is driven directly), and when $r_0 = \infty$, the mode is -1 (the neuron responds only when stimulus is missing). This yields the neural drive R_D,

$$R_D = 2^{1-r_0/r_0^*} - 1, \tag{2.1}$$

where r_0^* is the mean distance between the response and the last preceding stimulus spike if both stimulus and response were independent. If the stimulus spike train were periodic (with the standard deviation of the ISI distribution $\sigma = 0$), this distance would be $\frac{1}{2\lambda}$, while if the stimulus spike

train were Poisson distributed ($\sigma\lambda = 1$), it would be $\frac{1}{\lambda}$. Using $\sigma\lambda$ to scale between these two extremes, we get an expected distance of

$$r_0^* = \frac{1 + \sigma\lambda}{2\lambda}. \tag{2.2}$$

This theoretical value for r_0^* is accurate under the assumption that the stimulus is a mixture of regular and Poisson processes. If the stimulus has more complex time dependencies (e.g., is a sparse succession of fixed-length high-frequency bursts as in section 3.4), r_0^* should be computed numerically.

To achieve a range from -1 to 1 for the neural mode, the relative mean time interval of the last pair of stimulus spikes before the response, $r_1 = R_0 - R_{-1}$, is scaled exponentially so that when $r_1 = 0$, the mode is 1 (coincidence detection), when $r_1 = 1$ the mode is 0 (integration), and when $r_1 = \infty$, the mode is -1 (gap detection). This yields the neural mode R_M:

$$R_M = 2^{1-r_1/r_1^*} - 1. \tag{2.3}$$

2.3 Modes of Operation. To discern different modes of operation, we propose some boundaries in the $R_{M,D}$ plane (see Figure 2).

The neural drive R_D, based on the normalized distance r_0 of the last preresponse spike to the response, provides information on the timing of the response with respect to the stimulus trigger. Large values mean a response is fired relatively late, inside an unusually big gap in the stimulus spike train; small values mean a response is fired relatively quickly after the triggering stimulus. We suggest two boundaries to discern inhibition: independence and excitation. One border divides inhibition from independence, at $R_D = -0.1$. Values below $R_D < -0.1$ indicate that the mean response is triggered when there has been no stimulus for 115% longer than expected. The reference for this expectation is the mean interval that would be measured if stimulus and response were independent. If the presence of a response indicates the absence of stimulus, the stimulus in question has an inhibitory effect; hence, values of $R_D < -0.1$ indicate inhibition (see Figure 2, left column). Another border divides independence from excitation, at $R_D = 0.1$. Values between $R_D > -0.1$ and $R_D < +0.1$ indicate that the mean response is triggered at between 115% and 86% of its expected distance to the preceding stimulus. This area suggests independence (see Figure 2, middle column). Values of $R_D > 0.1$ indicate that the mean response is fired faster after the trigger than expected, at less than 86% of the independence reference value, suggesting excitation (see Figure 2, right column).

The neural mode R_M, based on the normalized distance r_1 of the two last preresponse spikes, provides information on the rate of the stimulus

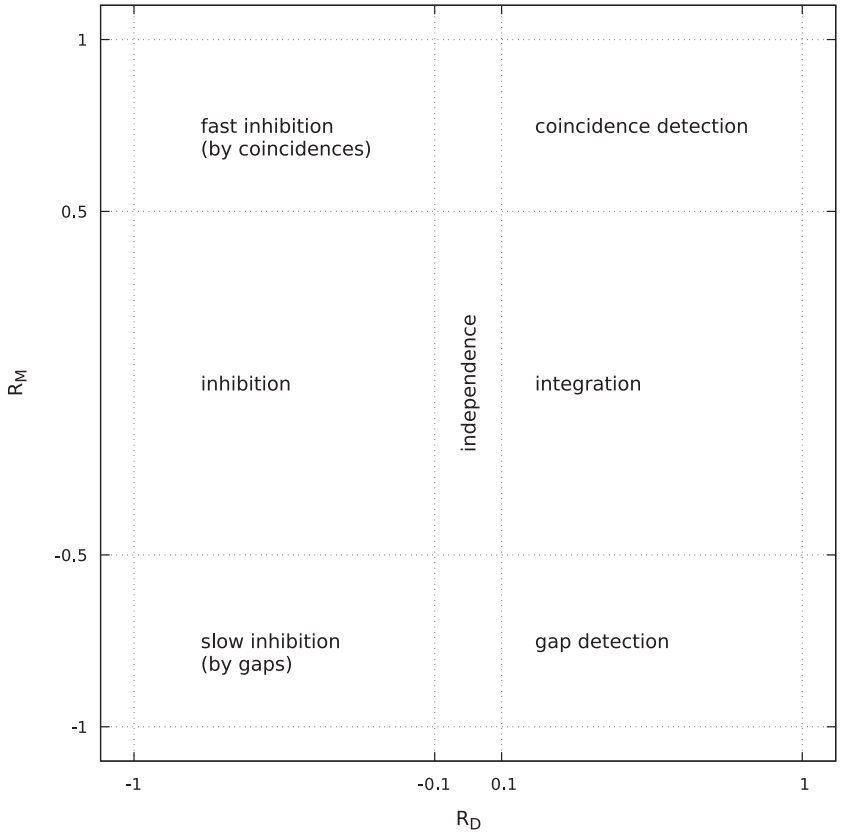

Figure 2: Overview of neural modes. The plane defined by the neural mode and the neural drive (see section 2.2 and equations 2.1 and 2.3). Areas are labeled according to the behavior of the responding neuron. For discussion, see section 2.3.

immediately before the response. Large values mean a response is a reaction to a drop in the stimulus rate (a gap in the stimulus), and small values mean a response is a reaction to a sudden increase in the rate (a coincidence). We suggest two boundaries to discern coincidence detection: temporal integration and gap detection. One border divides coincidence detection from integration, at $R_M = 0.5$. Values above $R_M > 0.5$ indicate that the mean response is triggered by a stimulus spike pair that is less than 42% wide, compared to its expected width. This corresponds to an increase in the local rate by a factor of 2.4. If a response indicates the presence of an unusually close spike pair, the response is marking a coincidence; hence, values of $R_M > 0.5$ indicate coincidence detection (see Figure 2, top row).

The other border divides integration from gap detection, at $R_M = -0.5$. Values between $R_M < 0.5$ and $R_M > -0.5$ indicate that the mean response reacts to stimulus spike pairs that are between 115% and 86% of their expected width apart. The response does not indicate any sudden changes of the local stimulus rate; this area suggests temporal integration (see Figure 2, middle row). Values of $R_M < -0.5$ indicate that the mean response is fired after a stimulus gap (in contrast to inhibition, where the response is fired inside a stimulus gap), with the preceding spike pair being more than 200% of its expected value apart, corresponding to a drop in the stimulus rate by a factor of 0.5. Values of $R_M < -0.5$ indicate gap detection (see Figure 2, bottom row).

Altogether, there are nine areas in the $R_{M,D}$ plane. On the inhibitory side, there is an area where a coincidence precedes a quiescence in stimulus (see Figure 2, top left). We have termed this fast inhibition. There is an area where the response is triggered by one quiescence in an otherwise normally paced stimulus (see Figure 2, middle left), and there is an area where the mean response is an answer to a general slowdown of the stimulus—at least one longer gap before the quiescence (see Figure 2, bottom left)—termed slow inhibition.

In the central column, there is an area where a response marks a coincidence, but the stimulus does not trigger the response directly (see Figure 2, middle top), an area where the response does not mark any change in stimulus at all (see Figure 2, middle), and an area where the response marks a gap in the stimulus but is not triggered directly (see Figure 2, middle bottom). These areas suggest independence, possibly in the coincidence, and in the gap detection case, there are indirect influences (populations, or connections via more than one neuron).

Within the area of excitation is an area of coincidence detection (see Figure 2, top right), defined by excitation and the detection of coincidences; an area of integration (see Figure 2, middle right), defined by excitation and the absence of coincidences; and an area of gap detection (see Figure 2, bottom right), defined by the detection of gaps in the stimulus.

3 Results

To explore the behavior of our new measure, several numerical simulations were carried out, as well as one experiment using publicly available recordings from a cat's cortex. All numerical simulations were run in C++ and NeuroLab.[1] The results are presented in this section; technical settings and parameters are described in the appendix.

[1] NeuroLab is an open source C++ class library for numerical simulation and analysis of stochastic processes in neuroscience, available online since 2005 and continually evolving. Source code and documentation can be downloaded from GitHub at https://github.com/jkanev/neurolab; precompiled packages are available on the first author's home page.

3.1 Corner Cases of the Measure. To demonstrate the measure on some corner cases, we used artificial spike trains and measured their $R_{M,D}$. No neuron was simulated; rather, stimulus and response time series were compared directly.

When a neuron responds to relatively closely arriving spikes within a slower spike train, and only then, we would say it is in a coincidence detection mode. The results of Figure 3, trace A, show the value for the neural mode R_M to be near 1; the value for the neural drive R_D is near 1 as well. In this case, the neuron separates coincidences from a noncoincident background.

In contrast, when a neuron receives only coincidences and responds to each one of them, it no longer separates coincidences from the background. The mean width of the spike pair preceding the response is close to the width that can be expected if the response were independent of the stimulus. This is because random independent events would most likely fall in between two coincidence pairs. Only in the unlikely case of a random event falling inside a coincidence pair does the preceding spike pair span the gap between two coincidences. The value for R_M is much nearer to zero (see Figure 3, trace B), so the neuron integrates over coincidences.

When a neuron responds regularly to regularly timed stimulus spikes, with a response directly after a stimulus, it is integrating. In agreement with this, the example in Figure 3, trace C, shows a value near zero for the neural mode R_M and a high neural drive R_D.

If a neuron is reacting only to stimulus pairs that are relatively wide apart compared to the mean time interval (e.g., because synaptic sensitivity is increased while the synapse is quiescent), we would say it is detecting gaps. Figure 3, trace D shows a sample train, and the resulting $R_{M,D}$ values show a negative value for the neural mode and a positive value for the neural drive (note that the response spike is emitted after the gap).

When a neuron's firing is independent of the timing of its stimulus, it shows a neural drive of zero, indicating independence. Our examples show two Poisson-distributed independent spike trains (see Figure 3, trace E) and two regular independent spike trains (see Figure 3, trace F). R_D is zero for both the regular and the irregular cases.

In the case of inhibition, the neuron does not respond directly after a stimulus spike, but a long time later, due to the suppressive effect of the stimulus (see Figure 3, traces H and I). In gap detection mode, the neuron responds directly after a stimulus spike, but only when there was a large gap before that last spike (see Figure 3, trace D). Inhibition occurs when the stimulating synapse has a very low reversal potential, while gap detection occurs when the synapse's sensitivity is increased by a quiescent stimulus.

3.2 Inhibition, Subthreshold, and Superthreshold Excitation. The biological mechanism for the excitation or inhibition of a neuron's response is the reversal potential of the stimulating synapse: stimulus at high reversal

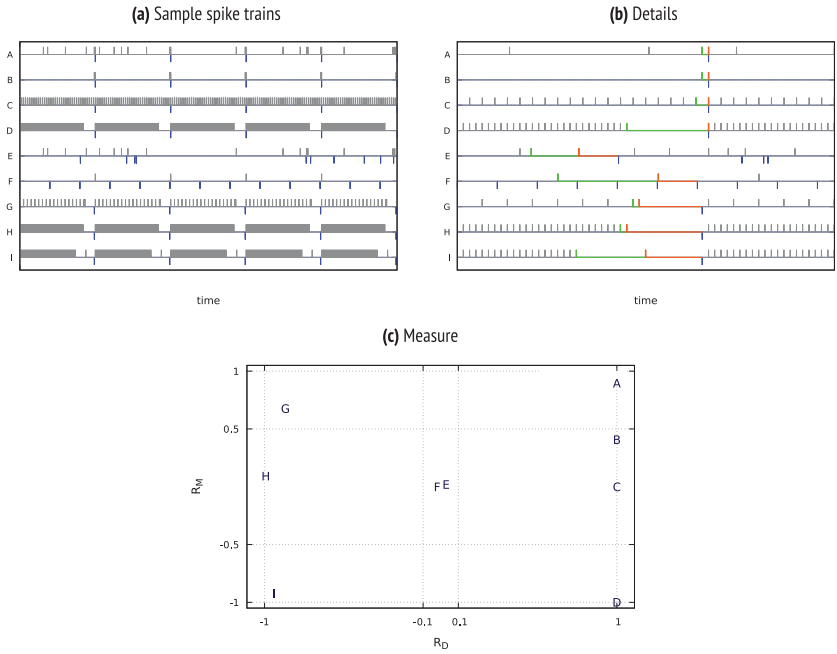

Figure 3: Corner cases of integration, gap detection and coincidence detection. (a) Artificial example spike trains. (b) Details of trains from panel a—one preresponse interval r_0 marked orange and the preceding interval r_1 marked green. (c) Measure in the $R_{M,D}$ plane. Spike trains: A, stimulus of coincidences within random stimulus; response at the coincidences: coincidence detection. B, stimulus of coincidences only; responses at the coincidence: integration over coincidences. C, regular stimulus, regular response: integration. D, stimulus with gaps, responses after gaps: gap detection. E, irregular stimulus, independent irregular response: independence. F, regular stimulus, independent regular response: independence. G, stimulus with coincidences followed by gaps, response during gap: fast inhibition. H, stimulus with gaps, response during gaps: inhibition. I, stimulus with successive gaps, response during gap: slow inhibition.

potential excites, and stimulus at low reversal potentials inhibits the response. The value of R_D reflects this behavior. To demonstrate this, we ran a numerical simulation using a leaky integrate-and-fire neuron model with conductances,

$$dV_t = \sum_i w_i \left(v_i - V_t\right) dG_t^i, \tag{3.1}$$

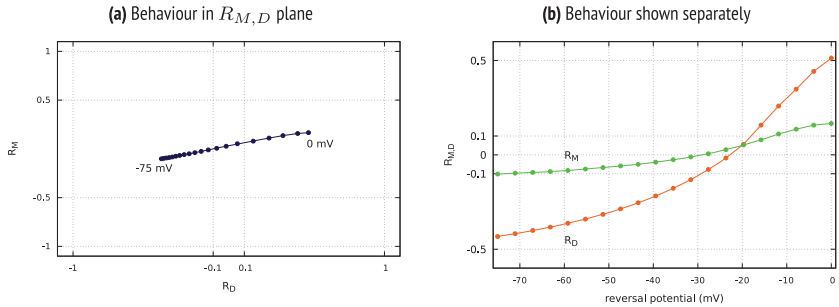

Figure 4: Mode and drive in relation to excitation versus inhibition. (a) Behavior of neural mode and drive ($R_{M,D}$) during the change of the signal synapse's reversal potential from −75 mV to 0 mV. (b) Behavior of neural mode (R_M) and drive (R_D) separately, in relation to the reversal potential.

where V_t is the membrane voltage, w_i are weights, v_i are reversal potentials, and dG_t^i are derivatives of stochastic processes (for parameter details, see section A.1). The results are shown in Figure 4. The neuron was driven by excitatory and inhibitory background noise and a signal, the reversal potential of which we changed in several runs. While changing the signal's influence on the neuron's response from excitatory to inhibitory, the neural drive reacts accordingly: an excitatory reversal potential corresponds to a neural drive $R_D > 0.0$, while an inhibitory reversal potential corresponds to a neural drive $R_D < 0.0$. While the reversal potential is changed and the neural drive value changes accordingly, the neural mode stays mostly unaffected.

A neuron can operate in two distinctly different regimes. In the subthreshold regime, the membrane potential mean is lower than the threshold, the neuron is driven by fluctuations in the membrane potential, and the neuron spikes with a lower rate and higher variance. In the superthreshold regime, the membrane potential mean is above the threshold, the neuron is driven by the membrane potential mean, and the neuron spikes with a higher rate and lower variance. The subthreshold regime is commonly associated with coincidence detection and the superthreshold regime with temporal integration (Kempter, Gerstner, & van Hemmen, 1998; Kempter, Gerstner, van Hemmen et al., 1998; Tchumatchenko, Malyshev, Geisel, Volgushev, & Wolf, 2010). The value of R_M reflects this. To demonstrate this, we ran a numerical simulation exploring different values of the membrane spiking threshold (see section A.2 for detailed parameter settings). The results (see Figure 5) clearly show that according to the value of R_M, the neuron used in the example integrates when in superthreshold regime and detects coincidences when in subthreshold regime. For any neuron, R_M will be higher when the neuron is in a subthreshold regime and lower when

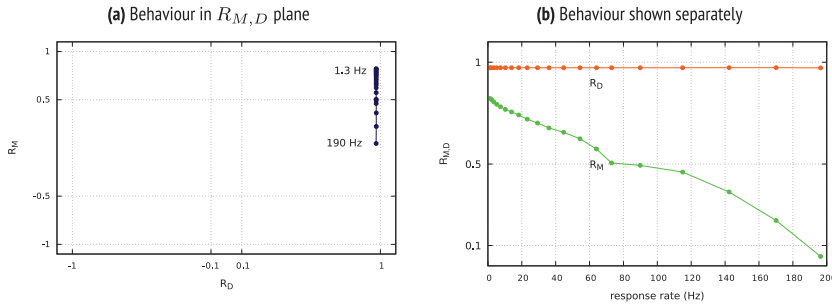

Figure 5: Mode and drive in relation to sub- versus superthreshold regime. (a) Behavior of neural mode and Drive ($R_{M,D}$) during the change of the regime from subthreshold to superthreshold. (b) Behavior of neural mode (R_M) and drive (R_D) separately, in relation to the response rate.

the neuron is in a superthreshold regime, although exact values of R_M may vary depending on other neural parameters. The kink in the R_M curve near $R_M = 0.5$ appears when the threshold is well above the mean membrane potential.

3.3 Comparison with Other Measures: Random Test. To compare our new measure with other measures that are used in the literature, we ran a numerical simulation using the same neuron model as before (conductance-based leaky integrate-and-fire; see equation 3.1). Between 100 and 150 trials were run and parameter values were chosen randomly (see section A.3 for technical details). We investigated the following measures:

1. The *normalised prespike slope* (NPSS, according to Koutsou et al., 2012). The original measure is based on a current-based neuron, in contrast to the conductance-based neuron model used in this study. Our calculation deviates from the original form as follows. For each response spike, a test neuron was created, and two membrane trajectories were calculated numerically—for ideal integration (the membrane potential reaches the threshold using a constant scalar stimulus) and for ideal coincidence detection (the neuron reaches the threshold because all stimuli are received within a 2 ms time window before the response). The actual voltage difference m in a 2 ms time window before the response was scaled by the respective values for the ideal integrator (m_{lower}) and the ideal coincidence detector (m_{upper}):

$$NPSS = \frac{m - m_{\text{lower}}}{m_{\text{upper}} - m_{\text{lower}}}. \tag{3.2}$$

2. The *coefficient of variation* (CV, used by Bell et al., 1995, and others) which in the current study we did not scale or normalise.

3. The *normalized coincidence advantage* (according to Abeles, 1982) shows the extent to which synchronous activation of a few synapses is more effective than asynchronous activation of the same synapses. A synchronous advantage a_C was obtained by calculating how many stimulus spikes would bring the membrane potential from its mean to the threshold v_θ,

$$a_C = \frac{1}{\lambda} \frac{v_\theta - \langle V_t \rangle}{v_S - \langle V_t \rangle}, \tag{3.3}$$

where v_S is the synaptic reversal potential of the synapses carrying the signal. Then the neuron was simulated without signal stimulus, only with background noise. Using r for the normal response rate measured previously and r_s for the response rate without stimulus, the integration advantage a_I is the gain of the response rate created by a single nonsynchronous stimulus spike,

$$a_I = \frac{r - r_s}{\lambda}. \tag{3.4}$$

The normalized coincidence advantage is the relation between the synchronous advantage a_C and the asynchronous advantage a_I:

$$a = \frac{1}{2} \frac{a_C}{a_I}. \tag{3.5}$$

4. For the *integration time window measure* (ITWM, according to König, Engel, & Singer, 1996) the membrane time constant was calculated, with the notable difference that the effective membrane time constant was used—that is, the effect of background noise on the time constant was taken into account. The result was exponentially scaled to achieve a value of 0 for pure integration and a value of 1 for pure coincidence detection:

$$ITWM = \exp\left(-\frac{r}{\frac{1}{\tau} + w_B \mu_B}\right). \tag{3.6}$$

Here r is the mean response rate, τ is the membrane time constant, w_B is the weight of the background synapses, and μ_B is the mean of the background stimulus rate. The expression $1/\left(\frac{1}{\tau} + w_B \mu_B\right)$ is the adjusted time constant, taking the change by the background noise into account.

These coincidence detection measures fall into two categories: membrane-based measures, like NPSS and integration time window

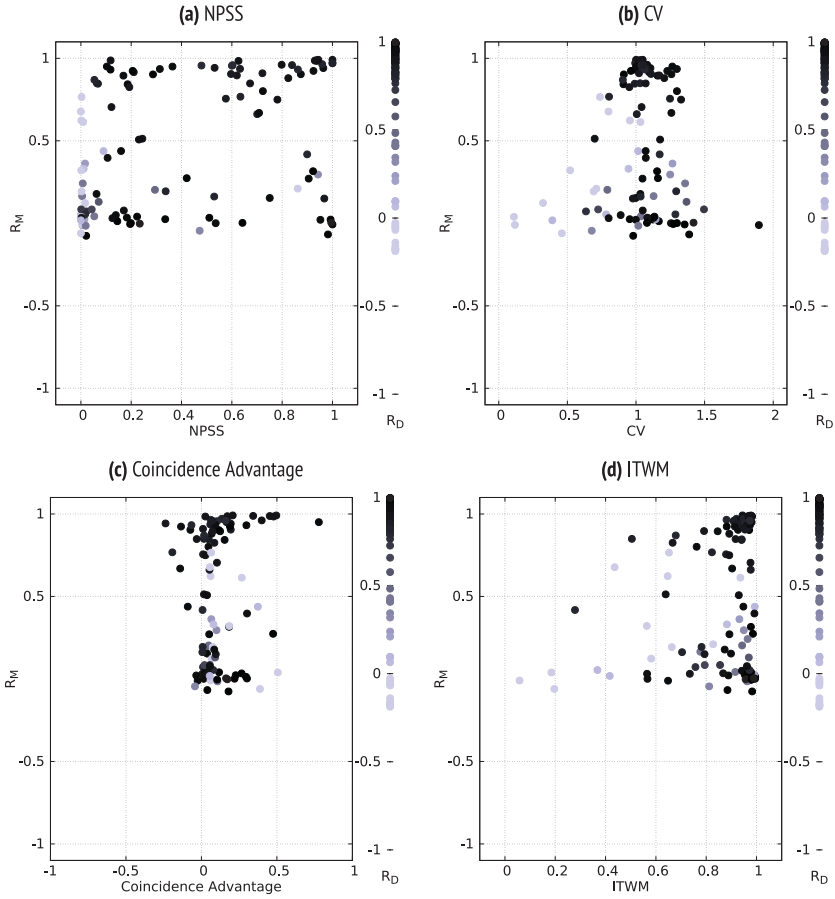

Figure 6: Comparison of neural drive and mode to different measures. (a) Comparison of NPSS and neural mode. $\rho_{x,y} = 0.035$. The Pearson correlation coefficient $\rho_{x,y} = 0.030$. (b) Comparison of coefficient of variation and neural mode, $\rho_{x,y} = 0.083$. (c) Comparison of the coincidence advantage according to Abeles (1982) and the neural mode. (d) Comparison of integration time window and neural mode, $\rho_{x,y} = 0.245$.

(ITWM), and pure spike-based measures like coincidence advantage, CV, and neural mode. Using a model neuron with random but biologically plausible parameter settings, we generated stimulus and response spike trains and assessed neural mode and drive. Figure 6 shows the value of each investigated measure plotted against the neural mode, where each point is the result of one simulation. No strong correlation can be seen between the

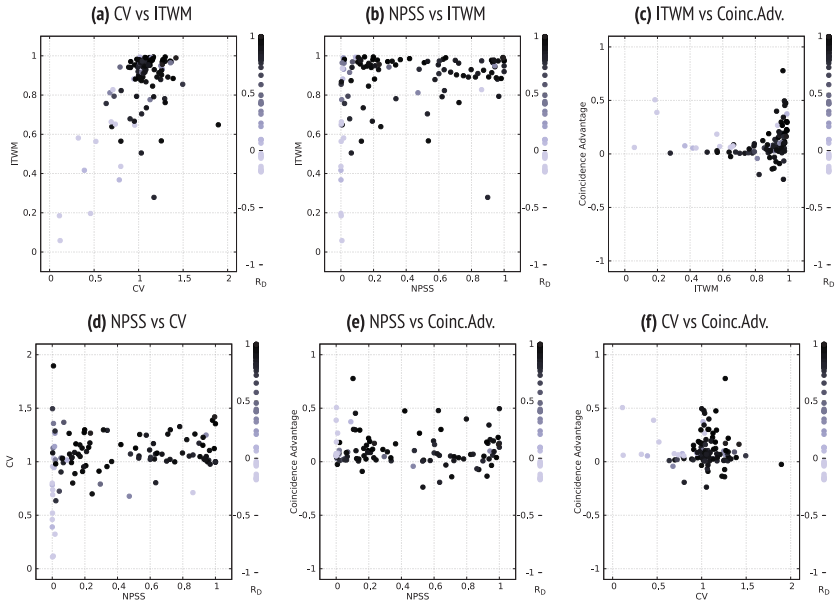

Figure 7: Pairwise comparison of different measures. (a) Comparison of coefficient of variation and integration time window; $\rho_{x,y} = 0.581$. Pearson correlation coefficient $\rho_{x,y} = 0.313$. (b) Comparison of NPSS and integration time window. (c) Comparison of integration time window and coincidence advantage, $\rho_{x,y} = 0.020$. (d) Comparison of NPSS and coefficient of variation, $\rho_{x,y} = 0.265$. (e) Comparison of NPSS and coincidence advantage, $\rho_{x,y} = 0.017$. (f) Comparison of coefficient of variation and coincidence advantage, $\rho_{x,y} = -0.202$.

neural mode and any of the other measures. Figure 7 shows the correlation of each measure with every other measure.

The plots suggest a correlation between the CV and the ITWM ($\rho_{x,y} = 0.581$; see Figure 7a), a weaker correlation between NPSS and ITWM ($\rho_{x,y} = 0.313$; see Figure 7b), and a weak nonlinear correlation of the ITWM and the coincidence advantage ($\rho_{x,y} = 0.020$; see Figure 7c). None of the tests show a really strong correlation between any of the tested measures. This suggests that each measure measures something different, as we explain below.

The NPSS measure is a measure based on the membrane potential. In contrast to all other measures, its calculation is response-interval based. It classifies the behavior of the membrane potential, placing it in a continuum between the two extremes of an integrator (a neuron spiking in response to totally scalar stimulus) and a coincidence detector (a neuron responding only when all input has arrived just before the response). It

operates on the complete system stimulus-neuron-response. A neuron receiving a regular stimulus and responding to each stimulus spike would be classified as a coincidence detector. The random test shows no relation to the neural mode but a relation to the neural drive (see Figure 6a). When a neuron is not directly driven by its input, it is classified as an integrator. The NPSS measures how the behavior of the membrane potential reflects synchrony in the stimulus. While a high NPSS measure is an indicator that a neuron might be detecting coincidences, a neuron might still react solely to coincidences and have a low NPSS, for example, when a stream of coincidences is responded to with a low response frequency (integrating over coincidences; see also Koutsou, Kanev, Economidou, & Christodoulou, 2016). Therefore we feel that the NPSS does not measure the neural mode directly, but is one of the means to achieve it. We found a weak correlation with the ITWM ($\rho_{x,y} = 0.313$; see Figure 7b), which is not surprising as both measures operate on preresponse time windows. The NPSS operates on a timescale defined by the length of the 2 ms preresponse window and the length of the response interval. The relationship between these lengths determines the neural mode, independent of the stimulus rate. This is in contrast to the other measures, and, in particular, the neural mode, which operates on a relative timescale defined by the stimulus. This explains the fact that there is no correlation of the NPSS with the neural mode.

Although it was never used as a direct measure of the neuron's operational mode, it was argued that a high CV (close to 1) in the case of high firing rates means that a neuron is not integrating (Softky & Koch, 1993). The CV is the only measure investigated that looks only at the response spike train. A neuron producing a regular response spike train (low CV) would be classified as an integrator, independent of whether it responds to regular close spike pairs or bursts, or not. Using the CV to classify a neuron makes sense only when the stimulus statistics are in a certain very narrow range, that is, when they show a Poisson-like distribution. The random test shows no relation to the neural mode but a relation to the neural drive (see Figure 6b). We also found a connection to the ITWM ($\rho_{x,y} = 0.581$; see Figure 7a). When a neuron is not directly driven by its input, the CV classifies it as integrator, although not as extremely as done by the NPSS measure. While a high CV can possibly be the result of coincidence detection, it is also conceivable that a high CV is the result of integration over short episodes of different stimulus rates or of bursting activity in the responding neuron. Therefore we think that the CV is a possible consequence of a certain mode of operation, with a weak connection to coincidence detection, even though other studies also show that integration is possible with a high response CV (Koutsou et al., 2012). The CV operates on a timescale defined by the neural response. Like the neural mode proposed in this letter, it is a relative measure, but the neural mode's timescale is determined by the stimulus. This is why there is no correlation between the two.

The ITWM states whether the neuron acts as a strong or a weak high-pass filter. Like the CV, it works independent of the stimulus and takes only the neuron's response into account. The results of the random test show a weak correlation to the CV, which suggests that time-based filtering and response CV are connected, but there is no correlation with neural mode or drive (see Figure 6b). The ITWM is a measure purely about the neural mechanism and independent of the characteristics of the stimulus. While a long integration time constant may hint at integration mode, it is still possible that due to balanced input, a neuron's membrane potential hovers near the threshold, making the neuron sensitive to coincidences. In that case, a neuron would be detecting coincidences, while the ITWM would classify it as an integrator. We feel that the ITWM, similar to the NPSS, does not measure the neural computation mode, but is a means to achieve it. The timescale the ITWM operates on is determined by the membrane time constant. In the way we conducted the simulation, this was influenced by the stimulus rate. Nevertheless, the timescale is absolute, while the timescale of the neural mode measure is relative. This explains the missing correlation between the two.

The coincidence advantage is the only measure that discerns signal and background within the stimulus. It operates on a neuron with random background input and measures how the neuron would react to an input signal on top of that background noise. It does not classify the complete system stimulus-neuron-response. An integrator is a neuron that treats a signal similar to background noise, while a coincidence detector is a neuron that uses its background to detect coincidences in its stimulus signal. The results of the random test show a weak correlation to the ITWM, which suggests a link between the idea of utilization of background noise for signal detection and the idea of filtering. There seems to be no relation to the neural mode, but a relation to the neural drive (see Figure 6c). It is biased toward coincidence detection and is the only measure that classifies neurons that operate independent of their stimulus as coincidence detectors. The coincidence advantage is a relative measure weighing how much a neuron amplifies a signal spike against a background stimulus. While related, this is a different concept of coincidence detection than any of the later proposed measures we found in the literature. The coincidence advantage uses an absolute timescale; in particular, it regards only those spikes as coincident that happen at exactly the same time. This is in contrast to the proposed neural mode and explains the missing correlation between neural mode and coincidence advantage.

3.4 Naturalistic Setting. A single incoming stimulus spike raises the neural membrane potential of a typical cortical neuron in vivo only by fractions of a millivolt. The density of stimulus is usually very high, and many stimulus spikes take part in raising the voltage to the threshold in the

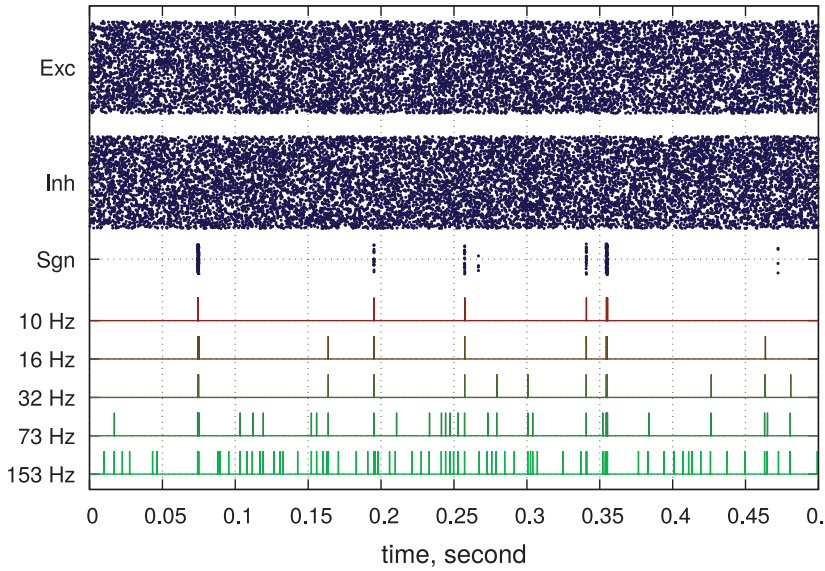

Figure 8: Neural mode in a realistic setting: Sample of stimulus and response. (Top to bottom) Exc: scatter plot of excitatory background stimulus spikes; each spike is one dot. Inh: scatter plot of inhibitory background stimulus spikes. Sgn: scatter plot of signal stimulus spikes, 10 Hz, 16 Hz, . . . , 153 Hz—responses of the five different neurons from the simulation. At 10 Hz, each response spike marks a signal spike packet. At higher response rates, spikes are increasingly caused by background fluctuations.

last milliseconds before the response. Our measure takes only the two very last stimulus spikes into account.

To test whether this approach is feasible in a realistic setting, we ran a numerical simulation of five leaky integrate-and-fire neurons with conductances linked to 5000 excitatory and 5000 inhibitory presynaptic background spike trains at 5 Hz each (see section A.4 for further details). In addition to that background, a signal consisting of 124 signal neurons where either 4, 20, or 100 neurons fired nearly simultaneously, with spikes $\frac{1}{100}$ ms apart, was added to the excitatory conductance. Each of the packets of 4, 20, or 100 spikes occurred with a rate of 3 Hz, adding up to a total of 9 Hz for the incoming spike packets. The five simulated neurons had different thresholds, making them respond at different rates. The first neuron fired at 10 Hz, picking up only the coincident spike packets in the signal and ignoring everything else. The second neuron fired at 16 Hz, in addition slightly responding to the background. The other three neurons fired at 32 Hz, 73 Hz, and 153 Hz, where the last neuron responded largely on the excitatory background (see Figure 8 for a sample of the spike trains). We analyzed

the result using the neural mode and drive. To get a complete picture, we measured how different parts of the input contribute in different ways to generate the observed response.

Looking at all the stimuli combined—excitatory, inhibitory, and signal—and measuring against the response, we find that the neuron that responds with 10 Hz performs coincidence detection, while the others are mainly integrating (see Figure 9g). This is in agreement with the fact that this neuron responds solely to the signal, while the other neurons also respond to the background, and it clearly shows how coincidence detection is used as a means to separate a weak signal from a strong background.

Looking at only the background, we find that the high-rate neurons operate as integrators on the background stimulus, while the low-rate neurons seem independent of the background. This is because they are driven by the signal and not by the background noise, and because inhibitory and excitatory effects of the background cancel out (see Figure 9d). Looking at only the excitatory stimulus and ignoring inhibition, the neural drive is much higher and coincidence detection is much more pronounced (see Figure 9f). Ignoring the excitatory background and analyzing only inhibitory background and signal, versus the response, leads to a result where the low-frequency neurons are coincidence detectors (responding to the signal), while the input to the high-rate neurons seems characterized by inhibition, meaning their response times are largely independent of the spike timing of the stimulus (see Figure 9e).

As expected, analyzing the effect of the excitatory background only results in integration for all neurons. This shows how neurons use integration on one part of their stimulus to become sensitive to another part (see Figure 9b). Also as expected, looking at the inhibitory background produces a similar result in the inhibitory range of the neural drive (see Figure 9c).

We measured how the signal itself influenced the neuron's response, neglecting the background. Because of the far-reaching temporal correlations (regular-spaced spike packets of up to 100 spikes, arriving in a random manner), the signal process is clearly not Poisson nor regular and cannot be estimated using equation 2.2. For this reason, we used a numerical estimation (see Figure 9a). As a comparison, we also show the regular/Poisson approximation of equation 2.2 (see Figure 9h). Interestingly, measuring how the neuron operates purely on the signal itself results in independence for the high-rate neurons (as expected) but in gap detection or integration for the low-rate neurons (see Figure 9a). The gap detection is a result of the structure of the stimulus. The neuron is so sensitive that it responds to the first spike of the stimulus spike volleys, thus detecting when the gap between the two volleys has finished. All this shows how coincidence detection can be used by a neuron to first separate signal from background and then process that separated signal using a different mode of operation (gap detection or temporal integration in our example). Here the neuron operates in a stochastic resonance scenario where background noise is used

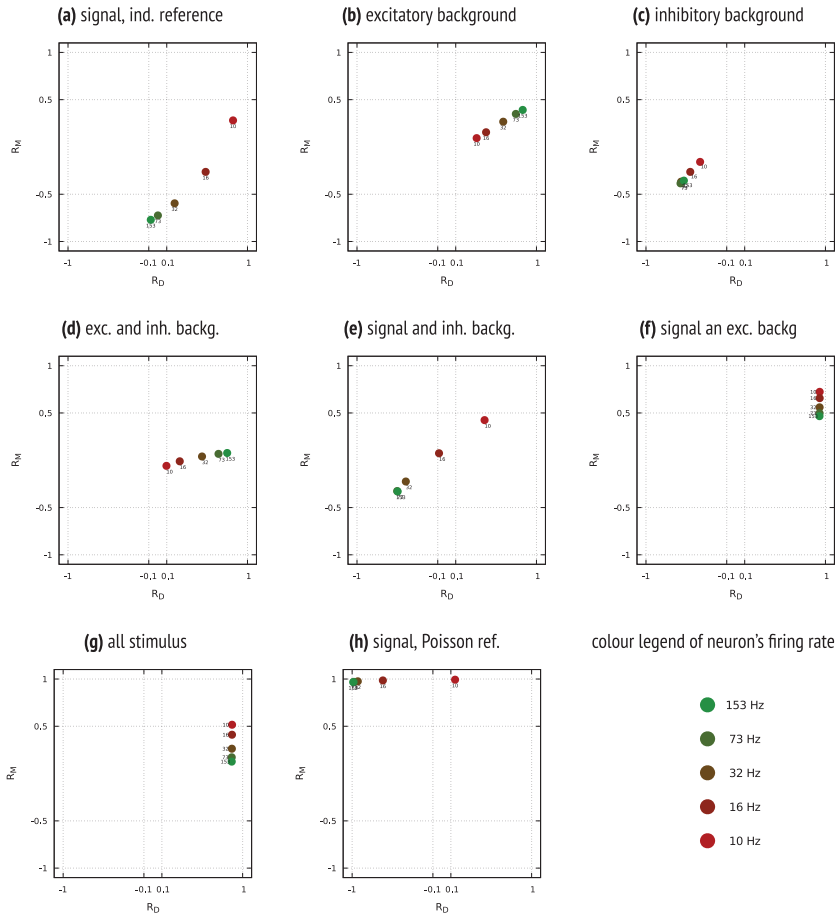

Figure 9: Neural mode in a realistic setting: Plane defined by $R_{M,D}$. (a) $R_{M,D}$ of signal versus response, using a numerical estimation for r_0^* in equation 2.1. (b) $R_{M,D}$ of excitatory background versus response. (c) $R_{M,D}$ of inhibitory background versus response. (d) $R_{M,D}$ of excitatory and inhibitory background combined versus response. (e) $R_{M,D}$ of signal and inhibitory background combined versus response. (f) $R_{M,D}$ of excitatory stimulus only (background and signal) versus response. (g) $R_{M,D}$ of all stimulus (excitatory, inhibitory, and signal) combined versus response. (h) $R_{M,D}$ of signal versus response, using a regular/Poisson calculation according to equation 2.2.

to achieve sufficient sensitivity to respond to small fluctuations in the signal (Plesser & Tanaka, 1997; Rudolph & Destexhe, 2001; Wenning & Obermayer, 2003).

3.5 Time Delay. An intrinsic problem of the way the new measure operates is that it relies on the immediate response after the last stimulus spike before that response: one single response spike is triggered by one single last stimulus spike occurring immediately before the response. This could pose a problem in the case of biological neurons where spike generation may take some time after being initiated. Stimulus occurring during this time would not contribute to the spike generation, but would be falsely identified by the new measure as stimulus that has triggered a response.

To overcome this problem we suggest calculating the neural drive and mode after adding a time delay d to each stimulus spike time. This time delay should match the time needed by the spike generation mechanism of the neuron. Unfortunately in most cases, d will not be known and can only be estimated. Here several measurements should be made using different values for d, and the value for d with the highest absolute drive should be used. This is the value that will most accurately fit the time distance between the last significant spike and the response.

Previous research has found that in the dendritic tree, active and passive properties counterbalance the different delay times caused by spatial distribution of the synapses. Depending on the location of the synapses, excitatory postsynaptic potentials (EPSPs) reach the soma with different amplitudes, but with no difference in time delay (Williams & Stuart, 2000; Magee, 2000). While it would be possible to find optimal time delay compensation values for spike trains on the basis of the spatial location of the respective synapses on the dendrite, we believe, on the grounds of mentioned research results, integration differences in the dendritic tree can be neglected.

To test the effect of less optimal values for d, we ran a numerical simulation with a conductance-based LIF neuron model as above, but with a delay after the threshold crossing to mimic the spike generation time. When the membrane potential V_t exceeds the threshold, the neuron is frozen for a small time period d and input stimuli during that time are ignored. After that time has passed, a spike is emitted and the neuron proceeds normally. In the simulation, we used the same background activity and neural parameters as in the naturalistic experiment (see section 3.4), except that there was no extra signal stimulus. Various studies have found a wide range of the first spike latency—values for pyramidal cells in the neocortex range from 0.32 ms (Waterhouse, Mouradian, Sessler, & Lin, 2000) to 137 ms (Kumar & Ohana, 2008). In our experiment, we used an arbitrary value for the spike generation delay of $d = 5$ ms. (see section A.5 for detailed parameter settings).

Figure 10a shows a sample of the neural membrane voltage. The voltage stays at the threshold for 5 ms before the spike is emitted. Figures 10b and 10c show the result with various values of d used in the analysis, while the delay of the tested neuron was always fixed. A delay in the analysis that matched the delay of the neural membrane turned out to be optimal and yielded

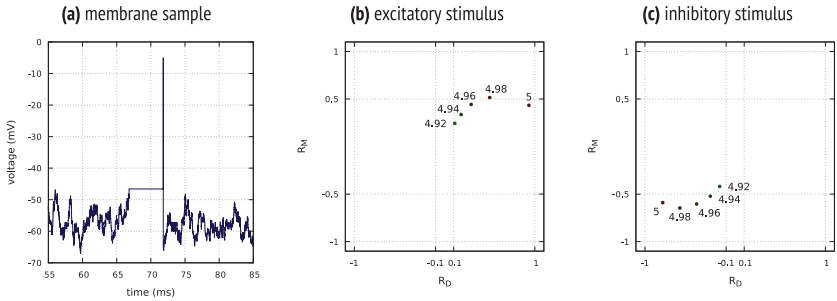

Figure 10: Time delay. (a) Membrane voltage sample, showing a threshold hit at 67 ms and subsequent freeze for 5 ms. (b) Calculated $R_{M,D}$ for the excitatory stimulus. Labels show different time delays of 5 ms to 4.92 ms. (c) Calculated $R_{M,D}$ for the inhibitory stimulus. Labels show different time delays of 5 ms to 4.92 ms.

the highest absolute drive in both the excitatory and the inhibitory cases. Delays that were slightly smaller reduced the neural drive, but increased the absolute neural mode. If the delay is too large, the causality is lost and the neural drive will equal zero (not shown).

The sensitivity of the neural drive and neural mode to time delay is proportional to the stimulus rate. As soon as several stimulus spikes get in between the last stimulus spike that has triggered the response, and the delayed response itself, the intervals r_0 and r_1 are calculated using the wrong stimulus spikes. An extreme case is a neuron responding to sparse single spike pairs in an otherwise evenly spaced stimulus spike flow. The causality is totally lost as soon as the neuron introduces a time delay that is larger than the stimulus rate. A more common case would be a neuron responding to spike volleys from a presynaptic neural population. Here the causality is lost only if the time delay is larger than the length of a spike volley.

Reducing the delay in the analysis shows a deterioration of both neural mode and neural drive to zero. The nonlinearity, that is, the rising of the neural mode in the excitatory and the falling in the inhibitory case, is a result of additional stimulus spikes being accounted for between the actual triggering spike and the response. In the case of excitation, if the delay time d is less than the mean distance of the last spike pair that triggered a response, additional spikes will produce a (wrongly accounted for) spike pair that is smaller than the actual one. Hence the neural mode will be slightly lifted toward coincidence detection. In the case of inhibition, the reverse of this effect takes place.

3.6 In Vivo Recordings. In this section, we demonstrate how the measure could be used to analyze data from in vivo measurements. Extracellular

recordings use multitrodes with several recording sites to record spikes that are produced in different local areas and are created by many different neurons. It is not clear whether recorded spikes are being used as inhibitory or excitatory stimulus by any postsynaptic neuron. It is also not clear whether a recording site has picked up the activity of a whole neural population, or just part of it, or activity from several populations. The approach we propose deals with this situation by combining one or several recording sites to sets and regarding each as a black box. The neural mode and neural drive are measured between pairs of black boxes. The combined spike train of one set's recording sites acts as a stimulus and the spike train of the other (usually single recording site) as response. The measure will indicate whether one group excites the other or inhibits it, whether coincidences trigger responses, or whether both groups are independent. That way, the ideas of temporal integration, coincidence detection, excitation, inhibition, and independence are applied to larger neural groups.

Different populations may be interconnected with a time lag due to their spatial separation. Our analysis is able only to apply fixed time lags per group. To find the optimal time lag compensation per neuron set, we explored five values between zero and 2 ms delay. An ideal analysis would measure each possible pair of subsets of recording sites against each other and explore many different time lags. Such an analysis was beyond the scope of this letter.

We used publicly available recordings from the NSF-funded CRCNS Data Sharing website (https://crcns.org/data-sets/vc/pvc-3). Neural data were recorded by Tim Blanche in the laboratory of Nicholas Swindale, University of British Columbia. We used the CRNS-PVC3 data set, which consists of several recordings from a cat's cortex done with a multitrode and one spike train for each of the multitrode's recording sites (more details are in section A.6). We do not make any statements about actual neural behavior in the mammalian cortex. We had no knowledge of the underlying neural connectivity or about how many neurons had contributed to the spike train from each recording site of the multitrode.

The data set contains several in vivo recordings in different situations. We measured each recording twice. In a first run, we measured all possible pairs of one response group consisting of a single recording site, and a stimulus consisting of all remaining recording sites (see Figures 11a to 11c). In a second run, we analyzed all possible triplets and measured the stimulus of two recording sites combined against the response of a third site (see Figures 11d to 11f). The analysis was done at different time lags, $d = 0, 0.5, \ldots, 2$ ms.

Figures 11a to 11c show mainly integration with a little bit of inhibition. Looking at all-to-one connections gives a very broad picture of what is going on inside a cortical column in total. If the dominant neural mode is integration, as it seems in our example, smaller subgroups showing other modes, like inhibition, would get lost.

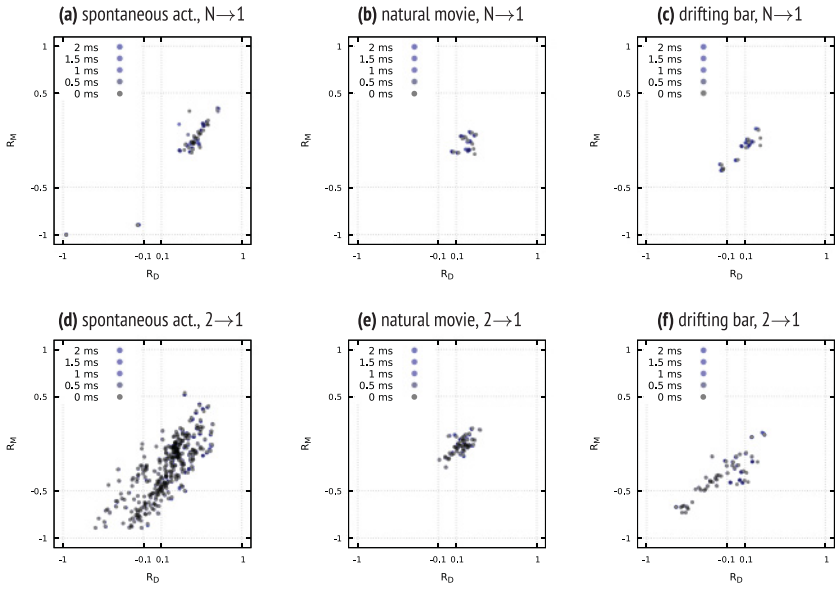

Figure 11: In vivo recordings of cat cortex. (Top row) All (N-1)-to-one electrode pairs. (a) Spontaneous activity in area 18. (b) Watching a natural movie. (c) Watching a drifting bar. (Bottom row) All two-to-one electrode pairs. (d) Spontaneous activity in area 18. (e) Watching a natural movie. (f) Watching a drifting bar.

Figures 11d to 11f show integration and slow inhibition but little coincidence detection. Looking at two-to-one connections gives a very detailed view of where each recording site will be measured against many possible stimulus pairs. Larger groups of signaling neural populations could get broken up, and, for example, a strong coincidence detection effect could be reduced in the analysis. Missing coincidence detection could be due to this fact or could simply not be present. Analysis also shows a high amount of slow inhibition: the response group responds only after the stimulus has slowed down for more than two spikes.

We explored various time delay values below 2 ms (the width of a spike of a typical CA2 pyramidal neuron; Scorza et al., 2011). Time delays below 2 ms had almost no effect on the neural mode and drive. The low sensitivity can be explained by two observations, the first being that the stimulus rate was below 500 Hz in all the measured groups, in both the two-to-one connections and all-to-one connections. Moving the response within a range of 2 ms would not change the intervals r_0 and r_1 a lot. The second observation justifying the low sensitivity was that none of the neurons was driven directly, with a neural drive $R_D \approx 1$. The interval r_0 was much larger

than 2 ms, and a time shift below 2 ms would have had little effect on its relative value R_0.

4 Summary and Discussion

4.1 Neural Mode and Drive. We believe the operational mode of a neuron should be the description of the mathematical operation of turning stimulus spikes into response spikes, independent of the physical nature of the computing neuron. An assessment of whether a response spike train is the result of coincidence detection or temporal integration should be possible to be made without knowledge of the producing neuron's inner working or the parameter settings of a certain model.

In this letter, we suggested a clear concept of coincidence detection, based entirely on spike trains. Coincidence detection is the mathematical operation of creating a response event time series where each response event marks a relative coincidence in the stimulus. We defined *coincidence* as two relatively close spikes compared to the rate of the spike train they occur in, and we defined *detection* as eliciting a response spike. This led to a spike-based definition of *excitation*, which we defined as responding to a stimulus faster than expected if stimulus and response were independent. To complete this, we also included *independence* as responding as fast as expected, *inhibition* as responding more slowly than expected, and *gap detection* as responding to two spikes that are relatively far apart.

These definitions lead to a two-dimensional measure $R_{M,D}$, where the neural mode R_M quantifies whether the eliciting events are coincidences, normally distanced spikes, or gaps, and where the neural drive R_D quantifies whether the response timing is excitatory, independent, or inhibitory (see equations 2.1 to 2.3).

4.2 Modes of Operation. Dividing the $R_{M,D}$ plane into several areas, we suggested different modes of neural operation. For a low value of the neural drive, near -1, when the neuron responds long after the last response spike was received, we have suggested *slow inhibition* (responding after the stimulus has died down for a bit), normal inhibition (responding as soon as the stimulus leaves a large gap), and *fast inhibition* (responding to an increase and subsequent silence of the stimulus). For a drive of zero, we have suggested *independence*, although the cases of a very high or a very low mode R_M are still interesting. In the case of high R_M, the neuron is reacting to coincidences among neurons to which it may be connected indirectly, while in the case of a low R_M, it may be sensitive to a signal with a special temporal structure (compare the simulation result in section 3.4, Figure 9a, for independent gap detection as a result of temporal correlations in the stimulus). For a high value of R_D, near 1, we have suggested *coincidence detection* (responding to coincidences in the stimulus, when R_M is also high), *integration* (responding, but not detecting particular patterns, when R_M is

near zero), or *gap detection* (responding to the first stimulus spike after a gap in the stimulus, when R_M is low).

4.3 Corner Cases of the Measure. We tested the behavior of the measure by applying it to extreme cases. Situations of perfect integration, perfect coincidence detection, gap detection, slow and fast inhibition, and two forms of independence were tested, and the resulting measure was in accordance with our theory.

4.4 Inhibition and Subthreshold and Superthreshold Excitation. Running numerical simulations, we also found that whether a neuron is in a subthreshold or a superthreshold regime is reflected by the neural mode. While all other parameters were fixed, applying the measure in a superthreshold regime resulted in integration; in a subthreshold regime, the result was coincidence detection. Looking at excitation or inhibition, the measure behaved as expected: subthreshold reversal potentials were classified as inhibitory, while superthreshold reversal potentials were classified as excitatory. A change of the reversal potential of a stimulating synapse results in a change of the neural drive, and changing the spiking threshold results in a change of neural mode.

4.5 Comparison with Other Measures. We compared the suggested measure with four selected measures from the literature and also compared these measures among themselves. We found some correlation, but no convincing agreement between any two measures. We have come to the conclusion that existing measures do not measure the operational mode of a neuron directly. As explained in section 3, they either quantify parameter settings or other mechanisms a neuron may use to execute a certain operational mode, or they quantify possible consequences of certain operational modes.

The CV measures the irregularity of a neuron's response. Under certain conditions, this can be an indicator of the neuron's operational mode. These conditions are quite restrictive: the stimulus must be a Poisson distributed flow of spikes with a static mean and variance and without any temporal correlations. The neuron's firing irregularity may be a possible consequence of the neural mode but not the neural mode itself. The coincidence advantage (CA) is a relative measure weighing how much a neuron amplifies a signal spike against a background stimulus and, in particular, at what distance to the threshold its mean membrane voltage lies. We believe the CA measures whether a neuron operates in a stochastic resonance scenario—or whether it does not. While these concepts are related, stochastic resonance is a result of coincidence detection, but both concepts are not identical. The integration time window measure (ITWM) measures whether a neuron works in a superthreshold or a subthreshold regime. The ITWM is a measure purely about the neural mechanism and independent of statistical

characteristics of the stimulus. The idea of the regime is related to the neural mode, but the ITWM does not measure the neural mode. The normalized prespike slope (NPSS) measures how the behavior of the membrane potential reflects synchrony in the stimulus. The idea to average the membrane potential slope before a response and the idea to average the last two stimulus spikes before the response are related. We believe the NPSS measures a biological mechanism—the use of the neural membrane as a high-pass filter—that is used to achieve coincidence detection or integration but not the neural mode itself.

Because of these slight differences of concept, none of the definitions from the literature we looked at are highly correlated between themselves. Moreover, apart from the CV, none of them is extendable to measure the spiking behavior of more abstract spike generators, like neural populations, artificial spike trains, or spike models that do not incorporate a neural membrane.

4.6 Naturalistic Setting and In Vivo Recordings. In the historic discussion of whether neurons act as integrators or coincidence detectors, there seems to be a consensus that a neuron operates somewhere in a continuum between these extremes (Koutsou et al., 2012, 2013; Ratté et al., 2015; Rudolph & Destexhe, 2003). There does not seem to be a consensus, though, on what the term *coincidence detection* actually refers to: a mode of a neuron only or a mode of a system consisting of stimulus, neuron, and response. We would argue that a neuron can use different neural modes at the same time, just as excitation and inhibition are used at the same time, depending on which subset of its stimuli is being investigated. An example would be a neuron operating in a stochastic resonance scenario and using integration on some of its input to enable it to execute either coincidence detection or gap detection on another part of its input. We propose the terms *neural drive* and *neural mode* to refer to a system consisting of a deliberately chosen subset of a neuron's stimulus and the neuron's response.

This modular approach enables an investigation of how stimulus groups that differ by a property like the reversal potential of their synapses are used differently by a responding neuron. By regarding the sources of a set of stimulus spike trains as a black box, analysis of relations between larger population becomes possible. It is conceivable to measure the combined stimulus spike train from one neural population against the combined response spike train from another population. A whole population may act as an integrator over the stimulus of another whole population or as a coincidence detector; populations may be excited or inhibited by the stimulus of other populations. A neuron inside a population may use coincidence detection to stay in sync with the firing of other population members, while at the same time, the whole population may be integrating over population-external background noise to get near a reaction threshold to start synchronous spiking.

The proposed measure takes only the two very last stimulus spikes before a response into account. In a typical high-density stimulus, many stimulus spikes may take part in raising the voltage to the threshold in the last milliseconds before the response. We still believe that looking at the last two spikes is sufficient. Averaging a small random sample over many trials to get information about the whole population is a common idea in statistical analysis. By constructing a measure from an average over just the two last spikes before a response, we apply that idea to the investigation into preresponse stimulus dynamics. Even if the elicitation of a response is done by a spike burst of several hundred spikes, the last two spikes will carry general information about spike timing and dispersion within the whole burst. By building an average of an interstimulus relation (the neural mode) and a stimulus-response relation (the neural drive) from these two spikes, we extract information about time dispersal within the burst, as well as information about the burst's relation to the response. Still, the approach is general enough to work in scenarios where a response is triggered by just one spike.

The experiment in section 3.4 was run to demonstrate both the concept of modularity and the idea that the last spike pair can serve as an estimator for the preresponse stimulus dynamics. We have measured the stimulus in seven groupings against the response of a single neuron. We believe the results clearly demonstrate the feasibility of the idea of grouping the stimulus into different larger sets and the idea of sampling by using just two spikes. The composition of the respective groups, and the way spikes were triggered, were well reflected in the final measure (see Figure 9 and text in section 3.4). The same idea was applied to an in vivo recording (see section 3.6), although a complete and extensive investigation into different groups and populations would have been outside the scope of this work.

A problem we have not addressed yet is the fact that in a high-density stimulus scenario, the last two spikes are very close together. The numerical simulation in section 3.4 was run with a time resolution of 2 nanoseconds. Measuring in *in vivo* or *in vitro* setups at such a resolution could be very demanding, if not unfeasible. There may be several ways to overcome this obstacle.

One way is to use prior knowledge about neural populations. If it can be assumed that a neuron receives a stimulus from a whole presynaptic neural population, the spike train of a small subgroup of that population may be used as an estimator for the whole group's stimulus-response relation with the neuron in question. The neural mode and drive from that small group's spike train would be measured against the response of the postsynaptic neuron. The small subgroup fires in the same way as the whole population, but with a much lower frequency. As the measure is independent of the actual stimulus rate, the value of neural mode and drive would be the same as for the entire population. To refine this approach, several such samples

could be taken and a total neural mode and drive built by averaging over those samples.

In a similar way, it is conceivable to use smaller, arbitrary subgroups of presynaptic neurons. However, in that case, the values of $R_{M,D}$ would have to be adjusted. To account for the fact that the responding neuron will respond to stimulus spikes that have not been recorded, the amount of (wrongly measured) independence has to be scaled down by a theoretical factor. This factor would depend on the total number of presynaptic neurons and the size of the subgroup.

Another, related approach would not look at small random samples in the spatial domain, but in the time domain. Instead of recording each stimulus spike, each nth stimulus spike (like each 10th or 100th) from the stimulus could be recorded. These times could also be calculated from a standard, lower-resolution recording where several spikes are recorded for the same time bin. As in the spatial estimation, the values of $R_{M,D}$ would have to be adjusted by a factor. Again, several such samples could be taken and a total neural mode and drive built by averaging.

4.7 Time Delay. The only way to determine a coincidence is by distinguishing it from steady background noise. Previously used measures use either an absolute timescale (ITWM, coincidence advantage) or a relative timescale that is based on the neural response (NPSS, CV). We think that the timescale used to distinguish coincidences from steady stimulus should be relative and based on the stimulus.

Although the measure itself is oblivious of any delay that might be present in the communication of the stimulating neurons and the responding neuron, if a delay is known or can be estimated by other means, we have shown that the time difference can easily be added to the response times of the response spikes when calculating the measure.

Previous research has found that there are no time delay differences caused by different spatial locations of EPSP generating synapses on the dendritic tree (Williams & Stuart, 2000; Magee, 2000). Depending on the location of the synapses, excitatory postsynaptic potentials (EPSPs) reach the soma with different amplitudes, but with no difference in time delay. It is therefore feasible to use one constant time delay to correct the anticausal effect of the dendritic integration time delay on the neural mode and drive.

In our examples, we have used a fixed timescale, either calculated theoretically using equation 2.2 or estimated numerically. Our proposed measure enables the researcher to use a dynamic timescale instead, for example, by computing the measure based on a sliding window with a fixed length of time or a fixed number of stimulus spikes, possibly multiplied with an exponential kernel. This will result in a time-changing value for neural mode and drive, and investigations into how a neuron changes its mode over time would become possible.

5 Outlook

In section 2.2 we proposed to define *coincidence detection* as responding to stimulus spikes that are close together, *integration* as responding to nonspecial stimulus widths, and *gap detection* as responding to gaps in the stimulus. We proposed to define *responding* as triggering a response spike unexpectedly quickly after a stimulus spike. From this definition we derived an exact measure $R_{M,D}$ for the neural mode and the neural drive (see equations 2.1 and 2.3) and suggested areas of coincidence detection, integration, gap detection, and slow and fast inhibition in the value plane of $R_{M,D}$ in section 2.3.

We believe our definitions and resulting measure have several advantages:

1. They are general in the sense that they are independent of the specific neuron model, or its parameters, or details of a real biological neuron to be measured. In fact, they are applicable to any way of generating response spikes from a stream of stimulus spikes by a biological neuron or a simulated neuron model, or any technical device, or a neural population, or they aid in the theoretical analysis of the relationship between stimulus and response.
2. They define a coincidence in the most general and intuitive way we can think of and do not rely on any time window parameters.
3. They allow the separation, independent analysis, and comparison of different groups of stimulating synapses, similar to the coincidence advantage introduced by Abeles (1982), only in a more general way. There is no fixed distinction between signal and background. Rather, the investigating scientist can define and analyze any grouping he or she wishes.
4. They are general in the sense that they cover all possible ranges of how a response can be influenced by the stimulus. A response can be elicited by coincident spikes, steady stimulus or gaps; response and stimulus can be independent, or suppressed by coincidences or steady stimulus or gaps.

These criteria of generality, simplicity, and truth to the concept make in our opinion our proposed measure favorable over previously used measures.

For future steps, we could think of using neural drive and neural mode for investigations into spike time series and the flow of time-related information between single neurons, populations, and regions in the brain. Here, distortions caused by interneural time delay should be taken into a account in more detail than we did in the scope of this work. It would also be interesting to conduct a thorough investigation into the mathematical properties of the new measure and into which parameters of different neuron and stimulus models influence neural mode and drive in which way.

We could also think of further investigations into how a neuron can achieve more complex ways of responding to its input by investigating how its response may be related to many different possible subsets of its stimulus by looking at both artificial settings and natural recordings. This was also beyond the scope of this study.

Appendix: Detailed Experimental Parameters

A.1 Inhibition and Excitation. Neural model parameters in the inhibition-excitation test in section 3.1 were: reset $v_0 = -65$ mV (partial reset according to Bugmann et al., 1997), membrane time constant $\tau = 45$ ms (Sanabria, Wozniak, Slusher, & Keller, 2004), resting potential $v_R = -80$ mV, three stimuli modeled by the derivative of a Poisson counting process—one excitatory background stimulus with rate $\lambda_E = 2000$ Hz, weight $w_E = 0.3$, reversal potential $v_E = 0$ mV, one inhibitory background stimulus with rate $\lambda_E = 2000$ Hz, weight $w_E = 0.3$, reversal potential $v_E = -75$ mV, one signal stimulus with rate $\lambda_S = 1000$ Hz, weight $w_S = 0.3$, and reversal potential in the interval $v_S \in (-75, 0)$ mV.

A.2 Subthreshold and Superthreshold Regime. Neural model parameters in the sub/superthreshold test in section 3.1 were: reset $v_0 = -65$ mV, membrane time constant $\tau = 45$ ms (Sanabria et al., 2004), resting potential $v_R = -80$ mV, two stimuli modeled by the derivative of a Poisson counting process—one excitatory background stimulus with rate $\lambda_E = 200$ Hz, weight $w_E = 0.2$, reversal potential $v_E = 0$ mV, one inhibitory background stimulus with rate $\lambda_E = 1000$ Hz, weight $w_E = 0.1$, reversal potential $v_E = -75$ mV. For each simulation run, the threshold was changed, ranging from -60 mV to -27 mV in 20 steps.

A.3 Comparison of Measures: Random Test. In section 3.3 we ran a numerical simulation using a conductance-based leaky integrate-and-fire (see equation 3.1). Between 100 and 150 trials were run, and parameter values were chosen randomly before each trial to cover all biologically plausible settings broadly: one excitatory signal conductance with weight $w_E \in (0, 0.5)$, reversal potential $v_E \in (-50, 20)$ mV; receiving spike pairs of distance $d \in (2, 200)$ ms, Poisson distributed, with rate $\lambda \in (2, 200)$ Hz; one inhibitory background conductance with weight $w_B \in (0, 1)$, reversal potential $v_I \in (-100, -20)$ mV, driven by white noise $\sigma_B * dW_t + \mu$ with mean $\mu_B \in (0, 1)$ and variance $\sigma_B^2 \in (1, 4)$; one leak conductance with a reversal potential $v_L \in (-70 + X, X)$ mV (where X is the maximum of the excitatory and the inhibitory reversal potential), and a response rate $r \in (2, 200)$ Hz, which was achieved by adjusting the threshold. Settings for which the effective membrane potential mean

$$\langle V_t \rangle = \frac{\sum w_i v_i \langle dG_t^i \rangle}{\sum w_i v_i}$$

was lower than the reset V_0 were rejected, as well as settings for which the reset V_0 was higher than the threshold, or when the resting potential v_L was above the threshold. Each trial lasted for 10,000 response spikes. After each run, the measures were calculated as described in section 3.3.

A.4 Naturalistic Setting. The numerical simulation in section 3.4 was run with a time step of $dt = 0.002$ ms to minimize the probability that two stimulus spikes fall into the same time bin.

Five conductance-based leaky integrate-and-fire neurons were simulated, with a reset potential of $V_0 = -80$ mV, a leak potential of $v_L = -80$ mV, a leak conductance density of $g_L = 0.045$ mS/cm^2, divided by a membrane capacitance of $C_m = 1$ μF/cm^2 resulting in a membrane time constant of $\tau = 22.22$ ms (Destexhe, Rudolph, Fellous, & Sejnowski, 2001). Each neuron had a unique threshold value, at $v_\theta = -44$ mV, -46 mV, -48 mV, -50 mV, -52 mV which led to response spike rates of 10, 16, 32, 73, and 153 Hz.

The numerical estimation for the value of r_0^* in equation 2.1 was made by calculating the mean distance of each event in an independent regular counting process with a rate of π10,000 Hz, to the nearest preceding signal spike.

The neurons were driven by:

- An excitatory Poisson process at a reversal potential of $v_E = 0$ mV, a synaptic weight of $w_E = 0.016$, and a rate of 25,000 Hz, representing 5000 inputs of neurons spiking at 5 Hz each,
- An inhibitory Poisson process at a reversal potential of $v_I = -75$ mV, a synaptic weight of $w_E = 0.055$, and a rate of 25,000 Hz, representing 5000 inputs of neurons spiking at 5 Hz each,
- A signal consisting of three kinds of coincidences, each arriving with a rate of 5 Hz and consisting of spikes $\frac{1}{100}$ ms apart—the first type consisting of 4 coincident spikes, the second of 20, and the third of 100 spikes.

The values for reversal potentials and weights used have been reported to mimic a natural cortical neuron most closely (Destexhe et al., 2001).

A.5 Time Delay. The simulation in section 3.5 was run with a time step of $dt = 0.002$ ms to minimize the probability that two stimulus spikes fall into the same time bin.

A conductance-based leaky integrate-and-fire neuron according to equation 3.1 was used, with a time-delayed spike response. After the voltage crosses the threshold, the computation of the next state of the neuron is stopped for a time period $d = 5$ ms. After this, a spike is emitted and the membrane voltage is reset to V_0.

The neuron was driven by an excitatory Poisson process at a reversal potential of $v_E = 0$ mV, a synaptic weight of $w_E = 0.016$, and a rate of

25,000 Hz, representing 5000 inputs of neurons spiking at 5 Hz, an inhibitory Poisson process at a reversal potential of $v_I = -75$ mV each, a synaptic weight of $w_E = 0.055$, and a rate of 25,000 Hz, representing 5000 inputs of neurons spiking at 5 Hz each. Values for reversal potentials and weights were used to mimic a natural cortical neuron most closely (Destexhe et al., 2001).

The neural drive and mode was calculated five times, each time adding a different value d to all stimulus spike times. Values were 5 ms, 4.98 ms, 4.96 ms, 4.94 ms, and 4.92 ms.

A.6 In Vivo Recordings. Neural data were recorded by Tim Blanche in the laboratory of Nicholas Swindale, University of British Columbia. Recordings were done using a politrode in an anesthetized animal. Spike data span roughly 300 seconds, in 10 to 50 recording sites (differing per recording). Further details can be found at CRCNS (https://crcns.org/data-sets/vc/pvc-3).

The time resolution when replaying the binary spike time files was 1 μs. Time resolution for the analysis was 0.5 ms.

Acknowledgments

We thank the two anonymous reviewers for their constructive and stimulating reviews.

References

Abeles, M. (1982). Role of the cortical neuron: Integrator or coincidence detector? *Israel Journal of Medical Sciences*, *18*, 83–92.

Bell, A. J., Mainen, Z. F., Tsodyks, M., & Sejnowski, T. J. (1995). Balancing of conductances may explain irregular cortical spiking. (Technical Report INC-9502). San Diego: Institute for Neural Computation, UCSD.

Bugmann, G., Christodoulou, C., & Taylor, J. G. (1997). Role of temporal integration and fluctuation detection in the highly irregular firing of a leaky integrator neuron model with partial reset. *Neural Computation*, *9*(5), 985–1000.

Destexhe, A., Rudolph, M., Fellous, J. M., & Sejnowski, T. J. (2001). Fluctuating synaptic conductances recreate in vivo–like activity in neocortical neurons. *Neuroscience*, *107*(1), 13–24.

Hsu, A., Borst, A., & Theunissen, F. E. (2004). Quantifying variability in neural responses and its application for the validation of model predictions. *Network: Computation in Neural Systems*, *15*(2), 91–109.

Kempter, R., Gerstner, W., & van Hemmen, J. L. (1998). How the threshold of a neuron determines its capacity for coincidence detection. *BioSystems*, *48*(1–3), 105–112.

Kempter, R., Gerstner, W., van Hemmen, J. L., & Wagner, H. (1998). Extracting oscillations. Neuronal coincidence detection with noisy periodic spike input. *Neural Computation*, *10*(8), 1987–2017.

König, P., Engel, A. K., & Singer, W. (1996). Integrator or coincidence detector? The role of the cortical neuron revisited. *Trends in Neurosciences*, *19*(4), 130–137.

Koutsou, A., Christodoulou, C., Bugmann, G., & Kanev, J. (2012). Distinguishing the causes of firing with the membrane potential slope. *Neural Computation*, *29*(9), 2318–2345.

Koutsou, A., Kanev, J., & Christodoulou, C. (2013). Measuring input synchrony in the Ornstein—Uhlenbeck neuronal model through input parameter estimation. *Brain Research*, *1536*, 97–106.

Koutsou, A., Kanev, J., Economidou, M., & Christodoulou, C. (2016). Integrator or coincidence detector: What shapes the relation of stimulus synchrony and the operational mode of a neuron? *Mathematical Biosciences and Engineering*, *13*(3), 521–535.

Kreuz, T., Chicharro, D., Andrzejak, R. G., Haas, J. S., & Abarbanel, H. D. I. (2009). Measuring multiple spike train synchrony. *Journal of Neuroscience Methods*, *184*(2), 287–299.

Kreuz, T., Chicharro, D., Greschner, M., & Andrzejak, R. G. (2011). Time-resolved and time-scale adaptive measures of spike train synchrony. *Journal of Neuroscience Methods*, *195*(1), 92–106.

Kreuz, T., Chicharro, D., Houghton, C., Andrzejak, R. G., & Mormann, F. (2013). Monitoring spike train synchrony. *Journal of Neurophysiology*, *109*(5), 1457–1472.

Kreuz, T., Haas, J. S., Morelli, A., Abarbanel, H. D. I., & Politi, A. (2007). Measuring spike train synchrony. *Journal of Neuroscience Methods*, *165*(1), 151–161.

Kreuz, T., Mulansky, M., & Bozanic, N. (2015). SPIKY: A graphical user interface for monitoring spike train synchrony. *Journal of Neurophysiology*, *113*(9), 3432–3445.

Kumar, P., & Ohana, O. (2008). Inter- and intralaminar subcircuits of excitatory and inhibitory neurons in layer 6a of the rat barrel cortex. *Journal of Neurophysiology*, *100*(4), 1909–1922.

Magee, J. C. (2000). Dendritic integration of excitatory synaptic input. *Nature Reviews Neuroscience*, *1*(3), 181–190.

Mainen, Z. F., & Sejnowski, T. J. (1995). Reliability of spike timing in neocortical neurons. *Science*, *268*(5216), 1503–1506.

Mulansky, M., Bozanic, N., Sburlea, A., & Kreuz, T. (2015). A guide to time-resolved and parameter-free measures of spike train synchrony. In *IEEE Proceedings of the 1st Int. Conf. on Event-Based Control, Communication, and Signal Processing Poland* (pp. 1–8). Piscataway, NJ: IEEE.

Ostojic, S., Brunel, N., & Hakim, V. (2009). How connectivity, background activity, and synaptic properties shape the cross-correlation between spike trains. *Journal of Neuroscience*, *29*(33), 10234–10253.

Plesser, H. E., & Tanaka, S. (1997). Stochastic resonance in a model neuron with reset. *Physics Letters A*, *225*, 228–234.

Ratté, S., Lankarany, M., Rho, Y.-A., Patterson, A., & Prescott, S. A. (2015). Subthreshold membrane currents confer distinct tuning properties that enable neurons to encode the integral or derivative of their input. *Frontiers in Cellular Neuroscience*, *8*, 452.

Roy, S. A., & Alloway, K. D. (2001). Coincidence detection or temporal integration? What the neurons in somatosensory cortex are doing. *Journal of Neuroscience*, *21*(7), 2462–2473.

Rudolph, M., & Destexhe, A. (2001). Correlation detection and resonance in neural systems with distributed noise sources. *Physical Review Letters*, *86*(16), 3662–3665.

Rudolph, M., & Destexhe, A. (2003). Tuning neocortical pyramidal neurons between integrators and coincidence detectors. *Journal of Computational Neuroscience*, *14*(3), 239–251.

Sanabria, E. R. G., Wozniak, K. M., Slusher, B. S., & Keller, A. (2004). GCP II (NAAL-ADase) inhibition suppresses mossy fiber-CA3 synaptic neurotransmission by a presynaptic mechanism. *Journal of Neurophysiology*, *91*(1), 182–193.

Scorza, C. A., Araujo, B. H. S., Leite, L. A., Torres, L. B., Otalora, L. F. P., Oliveira, M. S., . . . Cavalheiro, E. A. (2011). Morphological and electrophysiological properties of pyramidal-like neurons in the stratum oriens of Cornu ammonis 1 and Cornu ammonis 2 area of Proechimys. *Neuroscience*, *177*, 252–268.

Shadlen, M. N., & Newsome, W. T. (1994). Noise, neural codes and cortical organization. *Current Opinion in Neurobiology*, *4*(4), 569–579.

Shadlen, M. N., & Newsome, W. T. (1998). The variable discharge of cortical neurons: Implications for connectivity, computation, and information coding. *Journal of Neuroscience*, *18*(10), 3870–3896.

Softky, W. R., & Koch, C. (1993). The highly irregular firing of cortical cells is inconsistent with temporal integration of random EPSPs. *Journal of Neuroscience*, *13*(1), 334–350.

Stevens, C. F., & Zador, A. M. (1998). Input synchrony and the irregular firing of cortical neurons. *Nature Neuroscience*, *1*(3), 210–217.

Tchumatchenko, T., Malyshev, A., Geisel, T., Volgushev, M., & Wolf, F. (2010). Correlations and synchrony in threshold neuron models. *Physical Review Letters*, *104*(5), 5–8.

Waterhouse, B. D., Mouradian, R., Sessler, F. M., & Lin, R. C. (2000). Differential modulatory effects of norepinephrine on synaptically driven responses of layer V barrel field cortical neurons. *Brain Research*, *868*(1), 39–47.

Wenning, G., & Obermayer, K. (2003). Activity driven adaptive stochastic resonance. *Physical Review Letters*, *90*(12), 120602.

Williams, S. R., & Stuart, G. J. (2000). Site independence of EPSP time course is mediated by dendritic I(h) in neocortical pyramidal neurons. *Journal of Neurophysiology*, *83*(5), 3177–3182.

Received December 22, 2015; accepted May 2, 2016.